Nucleon-Nucleon Triplet-Even Potentials*

NORMAN K. GLENDENNING AND GUSTAV KRAMER†
Lawrence Radiation Laboratory, University of California, Berkeley, California

(Received December 26, 1961)

We have found a number of triplet-even potentials that fit the deuteron data, and yield scattering lengths falling within the rather large range of uncertainty of this quantity. The potentials behave at a large distance such as the one-pion exchange potential as required by meson theory. Potentials which fit the deuteron data and obey this asymptotic requirement can make a fairly unique prediction for the deuteron D-state probability if the triplet scattering length is accurately known. The phase shifts for our potentials have been calculated at 95, 210, and 310 Mev, and they fall within the range presently allowed by phase-shift analysis of the n-p data. The deuteron electromagnetic form factor was computed for some of the potentials, and the scalar nucleon form factor $F_1^n+F_1^p$ and neutron form factor F_1^n deduced from elastic electron-deuteron scattering data in the momentum transfer range $q\leqslant 3$ f^{-1}. This deduction depends, to a high degree of accuracy, only on the well-established one-pion exchange potential tail of the potential, and not on the inner region. We find that F_1^n is zero, or very small and negative.

I. INTRODUCTION

UNLIKE the situation for the p-p system, the experimental data on the n-p system are still not sufficient to specify the internucleon force in a more or less unique manner. However in the n-p system a triplet-even bound state exists whose properties serve as constraints on the force. In addition all meson theoretic derivations of nuclear potentials are in agreement on one further constraint: At large distance the nucleon potential must behave like the one-pion exchange potential (OPEP). Concerning the inner region, many different forms based on meson theory have been derived[1] but very little has been done to calculate the corresponding properties of the two-nucleon system.[2] The analysis of n-p data has been mostly done in terms of phenomenological potentials such as those constructed by Signell and Marshak,[3] by Gammel and Thaler,[4] and recently by Hamada.[5] However neither the Signell-Marshak nor the Gammel-Thaler potential fits the deuteron data while the latter in addition does not satisfy the OPEP constraint. On the other hand Hamada has been fairly successful in reproducing the deuteron properties and the n-p scattering data with potentials which do have OPEP tails. Hamada's potentials all give D-state probabilities for the deuteron larger than 7.5%. The D-state admixture is relevant to the magnetic moment, hyperfine structure, photodisintegration and the electromagnetic form factor of the deuteron. However it cannot be determined from experimental data yet due to unknown meson contributions to the electromagnetic interaction of the n-p system. The traditional limits considered to be appropriate have been $4\%<p_D<10\%$. It is, therefore, of interest to know whether information about p_D can be obtained from potentials that fit the known low-energy properties of the n-p system and behave asymptotically like the OPEP.

It was the purpose of the work described in this paper (a) to construct triplet-even potentials that are asymptotic to the OPEP and are modified in the inner region with ranges corresponding to the exchange of more than one pion in such a way that a bound state with the deuteron properties is obtained together with a phase shift at zero energy consistent with the known triplet scattering length; and (b) from these potentials to compute the D-state probability, the deuteron effective range, the shape-dependent parameter, scattering phase shifts for higher energies, and the deuteron electromagnetic form factor.

In principle the deuteron form factor, which can be measured by elastic electron-deuteron scattering, yields information about the triplet-even force. This source of information on the n-p force has not been exploited in much detail.[6,7] One expects the deuteron form factor to depend on the details of the inner region of its wave function for larger momentum transfer. We therefore illustrate how this form factor is affected by different assumptions for the inner region of the triplet-even potential. However, the deuteron form factor depends also on the charge parts of the neutron and proton form factors, and very weakly on the magnetic-moment parts of the neutron and proton form factors (except for large scattering angle). Therefore, at large momentum transfer we cannot obtain unambiguous information about the inner region of the potential unless we know the nucleon form factors, and conversely. Concerning the nucleon form factors, Hofstadter and co-workers have recently extended their measurements of the proton form factor to larger momentum transfer and deduced the neutron

* Work done under the auspices of the U. S. Atomic Energy Commission.

† On leave of absence from the University of Heidelberg, Heidelberg, Germany.

[1] For references to the original literature see Suppl. Progr. Theoret. Phys. (Kyoto), No. 3, (1956); M. J. Moravcsik and H. P. Noyes, Ann. Rev. Nuclear Sci. (to be published).

[2] J. M. Blatt and M. H. Kalos, Phys. Rev. **92**, 1563 (1953); S. Gartenhaus, *ibid.* **100**, 900 (1955).

[3] P. S. Signell and R. E. Marshak, Phys. Rev. **106**, 832 (1957).

[4] J. L. Gammel and R. M. Thaler, Phys. Rev. **107**, 1337 (1957).

[5] T. Hamada, Progr. Theoret. Phys. (Kyoto) **24**, 126 (1960); **25**, 247 (1961).

[6] V. Z. Jankus, Phys. Rev. **102**, 1586 (1956).

[7] J. A. McIntyre and S. Dhar, Phys. Rev. **106**, 1074 (1957): J. A. McIntyre and G. R. Burleson, *ibid.* **112**, 2077 (1958).

form factor from their proton results and from the inelastic electron-deuteron scattering data.[8] We have used these results for illustrative purposes in our deuteron form factors. However, for small momentum transfer the latter quantity depends almost solely on the tail of the potential, which is well established and can therefore be used to deduce the scalar nucleon form factor $F_1^n+F_1^p$. From the known value of F_1^p we can thus find the neutron-charge form factor F_1^n. Our results for F_1^n disagree with those of reference 8.

The method used to compute the deuteron properties corresponding to a given potential is the same as that of Hamada[5] and is briefly outlined in Sec. II. Section III contains the assumption about the form of the potential in the inner region, the empirical low-energy data, and a list of the forces that fit these data. In Sec. IV we give the calculated triplet-even phase shifts for the higher energies and compare them with recently published phase shifts obtained from an analysis of n-p scattering data.[9,10] The results for the deuteron form factor appear in Sec. V, together with a deduction of the neutron charge form factor.

II. SOLUTION OF THE DEUTERON PROBLEM

We assume that the deuteron can be described by a potential which contains a central, a tensor, and a spin-orbit part, i.e.,

$$V(r)=V_C(r)+V_T(r)S_{12}+V_{LS}(r)\mathbf{S}\cdot\mathbf{L}. \tag{1}$$

Let the S and D radial wave functions of the deuteron (multiplied by r) be $u(r)$ and $w(r)$. For a potential of the form (1) they are the solutions of the coupled equations

$$\begin{aligned} d^2u(r)/dr^2&=[U_C(r)+\alpha^2]u(r)+2\sqrt{2}U_T(r)w(r),\\ d^2w(r)/dr^2&=[6/r^2+U_C(r)-2U_T(r)-3U_{LS}(r)+\alpha^2]w(r)\\ &\quad+2\sqrt{2}U_T(r)u(r), \end{aligned} \tag{2}$$

where $\alpha^2\hbar^2=M\epsilon$, ϵ is the binding energy of the deuteron, M is the nucleon mass, and $U(r)=M/\hbar^2V(r)$.

From meson theory we know the form of the potential at large r, but the inner region cannot be derived unambiguously at present. Accordingly we regard this region as subject to phenomenological treatment. Finally we ensure that the solution of the differential equations (2) has the deuteron binding energy as an eigenvalue by making an appropriate choice for the radius of the repulsive hard core.

A method for solving this problem has been described and applied recently by Hamada.[5] For completeness we outline it briefly here again.

It is apparent that Eq. (2) has two sets of linearly independent solutions. As such we could choose (u_1,w_1) and (u_2,w_2) with the asymptotic requirement that the first solution has the behavior of an S function and the second behaves like a D function:

$$\begin{aligned} \begin{pmatrix}u_1\\ w_1\end{pmatrix}&\to\begin{pmatrix}e^{-\alpha r}\\ 0\end{pmatrix},\\ \begin{pmatrix}u_2\\ w_2\end{pmatrix}&\to\begin{pmatrix}0\\ e^{-\alpha r}[1+3/\alpha r+3/(\alpha r)^2]\end{pmatrix}. \end{aligned} \tag{3}$$

Starting with this behavior at a sufficiently large r, we integrate (2) inward to get the two solutions for arbitrary r. Then $u(r)$ and $w(r)$ are obtained as a linear combination of these two solutions:

$$\begin{pmatrix}u(r)\\ w(r)\end{pmatrix}=\frac{1}{(1+\eta^2)^{\frac{1}{2}}}\left\{\begin{pmatrix}u_1(r)\\ w_1(r)\end{pmatrix}+\eta\begin{pmatrix}u_2(r)\\ w_2(r)\end{pmatrix}\right\}. \tag{4}$$

The requirement that u and w in (4) vanish at the core radius r_c gives an equation for r_c which is solved by an interpolation procedure. The asymptotic D/S ratio η is then determined from

$$\eta=-\frac{u_1(r_c)}{u_2(r_c)}=-\frac{w_1(r_c)}{w_2(r_c)}. \tag{5}$$

The various static deuteron properties are obtained from solution (4) by simple integrations. Formulas for the deuteron effective range $\rho(-\epsilon,-\epsilon)$, the quadrupole moment Q, and p_D are given in the literature.[11] We adopt the usual relative phase of u and w used in reference 11.

III. TRIPLET-EVEN POTENTIALS

As emphasized earlier by many authors, the tail of the nucleon-nucleon potential is well known to be the one-pion exchange potential (OPEP):

$$V(\mathrm{OPE})=\mu\frac{f^2}{4\pi}(\boldsymbol{\tau}_1\cdot\boldsymbol{\tau}_2)\frac{e^{-x}}{x}\times\frac{1}{3}\left[(\boldsymbol{\sigma}_1\cdot\boldsymbol{\sigma}_2)+S_{12}\left(1+\frac{3}{x}+\frac{3}{x^2}\right)\right], \tag{6}$$

where $\lambda\!\!\!^{-}=1/\mu$ is the pion Compton wavelength, $x=\mu r$, and S_{12} is the tensor operator.

To the OPEP we add terms with ranges of $1/2\mu$ and $1/3\mu$ to account for the intermediate states of two and three pions. The complete ansatz for the central, spin-orbit and tensor parts of the triplet-even potential,

[8] R. Hofstadter, C. de Vries, and R. Herman, Phys. Rev. Letters **6**, 290 (1961); D. N. Olson, H. F. Schopper, and R. R. Wilson, *ibid.* 286 (1961); R. M. Littauer, H. F. Schopper, and R. R. Wilson, *ibid.* **7**, 141 (1961).

[9] M. H. Hull, K. E. Lassila, H. M. Ruppel, F. A. McDonald, and G. Breit, Phys. Rev. **122**, 1606 (1961).

[10] M. H. MacGregor, Phys. Rev. **123**, 2154 (1961).

[11] L. Hulthén and M. Sugawara, in *Handbuch der Physik* edited by S. Flügge (Springer-Verlag, Berlin, 1957), Vol. XXXIX, p. 69, Eq. (25.12); p. 70, Eq. (26.5); p. 86, Eq. (30.25).

including the OPEP is

$$V_C(r)=-\mu\frac{f^2}{4\pi}\left(\frac{e^{-x}}{x}\right)\left\{1+\frac{e^{-x}}{x}\left[a_1+\frac{a_2}{x}+\frac{a_3}{x^2}+\frac{a_4}{x^3}\right]\right\}, \quad (7a)$$

$$V_{LS}(r)=-\mu\frac{f^2}{4\pi}\left(\frac{e^{-x}}{x}\right)^2\left\{b_1+\frac{b_2}{x}+\frac{b_3}{x^2}+\frac{b_4}{x^3}\right\}, \quad (7b)$$

$$V_T(r)=-\mu\frac{f^2}{4\pi}\left(\frac{e^{-x}}{x}\right)\times\left\{\left(1+\frac{3}{x}+\frac{3}{x^2}\right)+\frac{e^{-x}}{x}\left[c_1+\frac{c_2}{x}+\frac{c_3}{x^2}+\frac{c_4}{x^3}\right]+\left(\frac{e^{-x}}{x}\right)^2\left[d_1+\frac{d_2}{x}+\frac{d_3}{x^2}+\frac{d_4}{x^3}\right]\right\}. \quad (7c)$$

Aside from the OPEP part, the dependence of $V_C(r)$, $V_T(r)$, and $V_{LS}(r)$ on x is completely arbitrary, and is suggested by perturbational-meson-theoretical calculations. For the spin-orbit force we have chosen $1/2\mu$ as the range, since there is no contribution to V_{LS} from the OPEP in the static approximation.

Cziffra and Moravcsik have attempted to determine the coupling constant $f^2/4\pi$ from neutron-proton scattering data.[12] However, we choose the value $f^2/4\pi=0.08$, in accordance with an analysis of pion-nucleon scattering.[13] For the pion Compton wavelength we take the value $1/\mu=1.415$ f.

We made an extensive search for potentials of the class represented by Eq. (7) by varying the coefficients a_i, b_i, c_i, d_i such that the quadrupole moment Q and scattering length a_t, would be near the empirical values. A recently reported value[14] for Q is $Q=(2.82\pm0.01)\times10^{-27}$ cm^2. Values for a_t given in the literature are $a_t=(5.415\pm0.012)$ f^{-1} (from Hulthén and Sugawara[15]) and $a_t=(5.39\pm0.03)$ f^{-1} (from Gammel[16]). On the basis of a new measurement of the coherent scattering length,[17] we calculated $a_t=(5.44\pm0.02)$ f^{-1}.

Potentials that fit these data are listed in the tables, those without a spin-orbit term in Table I, and two potentials with a spin-orbit term in Table II. The last column in each of those tables contains the hard-core radius chosen so that the potential has a bound state with the eigenvalue $\epsilon=2.226$ Mev ($\alpha=0.2317$ f^{-1}). For the potentials listed in Tables I and II we have calculated the following additional deuteron properties: the asymptotic ratio of the D to S function, called η; the D-state probability p_D; the deuteron effective range $\rho(-\epsilon,-\epsilon)$; the normalization constant N^2, which is related to ρ by

$$N^2=2\alpha/[1-\alpha\rho(-\epsilon,-\epsilon)], \quad (8)$$

[where $N^2\int(u^2+w^2)dr=1$]; and the shape-dependent parameter P_t derived from a_t, ρ, and α by

$$P_t=\frac{1}{\alpha^3\rho^3}\left(\frac{1}{\alpha a_t}+\tfrac{1}{2}\alpha\rho-1\right). \quad (9)$$

TABLE I. Potentials without a spin-orbit force. (Parameters not mentioned in the table are zero.)

No.	a_1	c_1	c_2	c_3	c_4	d_1	d_2	d_3	r_c (f)
1	0.0	0.0	0.0	0.0	0.0	0.0	0.0	0.0	0.4815
2	1.0	3.0	0.0	−4.8	0.8	0.0	0.0	0.0	0.2466
3	8.0	−0.4	−1.2	−1.2	0.0	0.0	0.0	0.0	0.4747
4	0.5	−0.15	−0.45	−0.45	0.0	0.0	0.0	0.0	0.4425
5	1.0	−0.1	−0.3	−0.3	0.0	−0.2	−0.6	−0.6	0.3632
6	1.0	0.4	1.2	1.2	0.0	−0.8	−2.4	−2.4	0.3924
7	10.0	−3.0	0.0	0.0	0.0	0.0	0.0	0.0	0.5369

The OPEP gives a quadrupole moment $Q=2.879\times10^{-27}$ cm^2 and scattering length $a_t=5.378$ f^{-1}, which are not far from the experimental values, and the D-state probability is 7.4%. By modifying the inner region according to our ansatz, we sought to obtain simultaneously the correct Q and a_t. First we want to note that modifications of the potential at short range [$r\lesssim(2\mu)^{-1}$] cannot be expected to cause large changes from the OPEP values of Q, a_t, and p_D because the deuteron, being a loosely bound structure, feels the inner region very little. Its radius already exceeds the OPEP range (i.e., $P_t\approx0$)! It just happens to be one of the quirks of nature that the force that binds the deuteron does so in such a way as not to reveal itself too intimately through the properties of that structure. Nonetheless, because of the paucity of n-p scattering data, we are left with the task of gleaning from the deuteron what information we can about the triplet-even force.

As Table III shows, it is possible to modify the OPEP in a number of ways to obtain agreement with Q and a_t. However, it was not possible to fit these two data with a potential that yields a p_D much lower than the value that OPEP gives. This can be understood as follows:

TABLE II. Potentials with a spin-orbit force. (Parameters not mentioned in the table are zero.)

No.	a_1	a_4	b_3	b_4	c_1	c_2	c_3	c_4	r_c (f)
8	0.0	3.0	0.0	2.0	5.0	−5.0	−1.0	0.0	0.5007
9	3.0	0.0	−2.0	0.0	−0.4	−1.2	−1.2	0.0	0.4329

[12] P. Cziffra and M. J. Moravcsik, Phys. Rev. **116**, 226 (1959).
[13] T. D. Spearman, Nuovo cimento **15**, 147 (1960); Nuclear Phys. **16**, 402 (1960); G. Breit, M. H. Hull, K. Lassila, and K. D. Pyatt, Phys. Rev. Letters **4**, 79 (1960).
[14] G. P. Auffray, Phys. Rev. Letters **6**, 120 (1961).
[15] L. Hulthén and M. Sugawara, reference 11, p. 51 (footnote).
[16] J. L. Gammel, *Fast Neutron Physics*, edited by J. B. Marion and J. L. Fowler (Interscience Publishers, Inc., New York), Vol. IV, part II.
[17] L. Passel, W. Dickinson, W. Bartolini, and O. Halpern, Lawrence Radiation Laboratory Report UCRL-6320 (unpublished).

TABLE III. Low-energy properties of the potentials 1–9.

No.	Q ($\times 10^{27}$ cm^2)	a_t (f^{-1})	η	p_D (%)	ρ (f^{-1})	N^2 (f^{-1})	P_t
1	2.879	5.376	0.02714	7.415	1.717	0.7694	0.028
2	2.821	5.368	0.02693	6.281	1.709	0.7671	0.032
3	2.817	5.456	0.02595	5.970	1.812	0.7986	0.013
4	2.822	5.364	0.02677	7.103	1.703	0.7655	0.031
5	2.802	5.366	0.02663	6.710	1.705	0.7661	0.032
6	2.812	5.384	0.02676	5.957	1.726	0.7723	0.026
7	2.814	5.477	0.02564	6.029	1.836	0.8065	0.009
8	2.818	5.413	0.02654	5.622	1.7602	0.7826	0.018
9	2.829	5.373	0.02670	7.425	1.715	0.7690	0.031

Because of the large radius of the deuteron, the *shape* of the D function is *almost* independent of the inner region of the potential. However, its magnitude is proportional to η (and hence p_D to η^2). Now, to fit both Q and a_t, it is necessary that a more or less unique value of η obtains, as we now show. Since the quadrupole moment is weighted by r^2, we can calculate it approximately from the asymptotic part of the wave functions, Eq. (3):

$$\frac{10(1+\eta^2)Q}{\sqrt{2}N^2}\simeq\eta\int u_1w_2r^2dr-\frac{\eta^2}{2\sqrt{2}}\int w_2^2r^2dr. \quad (10)$$

From Eq. (10) it follows that η is given in terms of Q, N^2, and integrals that are asymptotically independent of the force. Since our earlier remark implies $P_t\approx 0$, N^2 is determined by the scattering length a_t from Eqs. (8) and (9).

Thus it is approximately true that potentials with OPEP tails which give the correct low-energy properties will all yield about the same D-state probability for the deuteron.

Nevertheless we constructed potentials with a D-state probability somewhat lower than 7% which are acceptable because they reproduce the zero-energy scattering with a scattering length consistent with the rather large range of experimental values mentioned earlier. The results shown in Table III suggest that a larger a_t would lead to a smaller p_D, consistent with the discussion above in connection with Eq. (10). From this point of view a knowledge of the correct value of a_t is very important.

It is noteworthy that the recently published value for the quadrupole moment,[14] which is higher than had previously been thought, results in a larger η and therefore higher p_D.

Concerning the D-state probability, the final conclusion of our investigation is that a triplet-even potential that has the correct asymptotic behavior and yields the deuteron binding energy and quadrupole moment will permit an almost unique prediction for p_D if the triplet scattering length a_t is accurately known.

The potential No. 6 has a special property compared to the others. At a very small radius ($r\simeq 0.75$ f) the D-state function has a node. The D function will develop a node even though this corresponds to a greater kinetic energy and might be expected at first to be an excited state, whenever the tensor force has a sufficiently strong "repulsive" singularity. For, in this event as can be seen by examining the wave equation (2), the repulsion can be turned into attraction by a change in sign of the D function, thus increasing the potential energy. Even the presence of the node at small r, however, does not appreciably change the function at larger r, in the sense that the low-energy properties (see Table III) are within the range of variation exhibited by the properties of the other potentials.

The effect of adding a spin-orbit force of negative and positive sign can be seen from Table III. The negative spin-orbit potential, which appears as a repulsion in the wave equation (2), decreases, whereas the opposite sign increases p_D.

IV. n-p SCATTERING PHASE SHIFTS

There exist phase-shift analyses of n-p scattering data by two groups. Hull *et al.*[9] have analyzed the data up to 300 Mev, while MacGregor[10] has analyzed the 95-Mev data. Both groups used the phase shifts for the isotopic spin $T=1$ states found from earlier analysis of p-p scattering. In the n-p analysis by Hull *et al.*, several phase-shift solutions were obtained, while MacGregor found only one solution at 95 Mev. However the experimental data are not sufficiently abundant to assure that even other solutions do not exist. Thus there does not exist a set of phase shifts for the $T=0$ state that is in any sense as "unique" as for the $T=1$ state. Nevertheless it is worth while to discover which of our potentials

TABLE IV. Phase shifts for triplet-even state.

No.	δ_{01}	δ_{21}	ϵ_1	δ_{23}	δ_{43}	ϵ_3	δ_{22}
			$E=95$ Mev (lab)				
1	0.8074	−0.2410	0.04373	0.06040	−0.06748	0.6843	0.3629
2	0.8355	−0.2341	0.01476	0.06341	−0.06842	0.6771	0.3548
3	0.7451	−0.2165	0.05797	0.07606	−0.05699	0.5937	0.3817
4	0.8258	−0.2335	0.03537	0.06033	−0.06659	0.6809	0.3506
5	0.8287	−0.2304	0.03001	0.06139	−0.06607	0.6756	0.3482
6	0.8158	−0.2316	0.01501	0.06376	−0.06727	0.6720	0.3658
7	0.7235	−0.2110	0.07633	0.07950	−0.05323	0.5678	0.3908
8	0.7649	−0.2378	0.02288	0.07947	−0.06125	0.5952	0.3524
9	0.8315	−0.2226	0.04747	0.05879	−0.06610	0.6883	0.3632
			$E=210$ Mev (lab)				
1	0.3579	−0.4576	0.06384	0.1269	−0.1335	0.5726	0.7173
2	0.4237	−0.4258	−0.01283	0.1313	−0.1357	0.5657	0.6345
3	0.2886	−0.3928	0.1119	0.1708	−0.1064	0.4673	0.7218
4	0.3897	−0.4378	0.04815	0.1244	−0.1305	0.5710	0.6780
5	0.3988	−0.4274	0.03302	0.1271	−0.1293	0.5648	0.6566
6	0.4076	−0.4106	−0.04897	0.1383	−0.1340	0.5560	0.6723
7	0.2597	−0.3910	0.1674	0.1819	−0.0974	0.4406	0.7624
8	0.2953	−0.4386	0.01125	0.2595	−0.1055	0.3538	0.6243
9	0.4153	−0.4041	0.08872	0.1092	−0.1314	0.6157	0.7163
			$E=310$ Mev (lab)				
1	0.1037	−0.5989	0.08947	0.1696	−0.1752	0.5029	0.8803
2	0.2021	−0.5357	−0.03307	0.1685	−0.1763	0.4966	0.7410
3	0.03847	−0.5031	0.1826	0.2287	−0.1350	0.4008	0.8539
4	0.1450	−0.5683	0.06821	0.1639	−0.1699	0.5025	0.8329
5	0.1596	−0.5493	0.04304	0.1670	−0.1679	0.4961	0.7947
6	0.2275	−0.4910	−0.1614	0.1853	−0.1761	0.4844	0.7799
7	0.00937	−0.5163	0.2750	0.2454	−0.1235	0.3805	0.9042
8	0.02711	−0.5602	0.00953	0.4883	−0.1279	0.1993	0.7209
9	0.1928	−0.5142	0.1436	0.1307	−0.1724	0.5828	0.8854

give phase shifts similar to those obtained from the analyses mentioned above.

Accordingly we have calculated the phase shifts $\delta_{\lambda J}$, ($\lambda = J \pm 1$) and coupling parameter ϵ_J at 95, 210, and 310 Mev for the $J=1$, 2, and 3 states. The phase shifts for the coupled states are obtained according to the Blatt-Biedenharn definition.[18] The results are listed in Table IV.

We now discuss some of the general properties of these phase shifts. The shifts for the larger angular momenta ($^3D_2$,$^3D_1$,$^3G_3$) are rather independent of the form of the inner region of the potential even for 300 Mev. Of course the $^3S_1$ phase shift depends very much on the details of the potential in this region and is affected most strongly by the different values of the hard-core radius r_c. A large r_c corresponds to a small $^3S_1$ phase shift. The coupling parameter in the state with $J=1$ is rather small, and is an increasing or decreasing function of energy depending on the details of the potentials. The spin-orbit force of negative sign (potential No. 8) causes the $^3D_2$ phase to increase less with energy than the others, as can be understood by an examination of the differential equation (2).

The phase shifts for $J=3$ are in general small except for potential No. 8, which has a larger $^3D_3$ phase at 310 Mev. The coupling parameter ϵ_3 is positive and very large in the Blatt-Biedenharn definition.

How all the phase shifts are affected by the details of the inner region of the potential can be seen by a comparison with the phase obtained for the OPEP (No. 1) modified by a suitable hard core.

In Figs. 1, 2, and 3 we have plotted the range in which our phase shifts fall, together with the phases obtained by an analysis of the experimental data by Hull *et al.*[9] and MacGregor.[10] The phase of Hull *et al.* were read from their graphs at laboratory-system energies of 100, 200, and 300 Mev and converted into Blatt-Biedenharn phases. We have illustrated the only two solutions that resemble the phases calculated from our potentials. (These two solutions are denoted by YLAN1 and YLAN3 in reference 9.) The phases δ_{01}, δ_{21}, ϵ_1, δ_{23}, and δ_{43} are in quite good agreement with the data analysis. However, the phase shift δ_{22} rises too steeply with

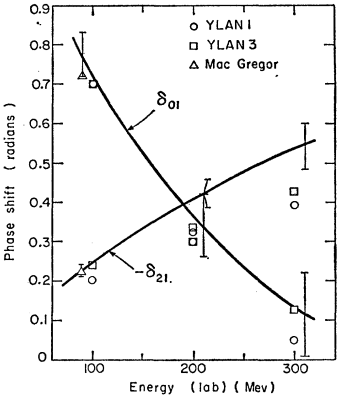

FIG. 1. The coupled phase shifts δ_{01} and δ_{21}, computed from the potentials listed in Table I, are illustrated by indicating with a vertical bar the range in which they fall at three energies. The centers of these ranges are joined by a smooth curve. Two phase-shift solutions of the analysis of the data by Hull *et al.* are shown (referred to in their notation as YLAN 1 and YLAN 3), together with MacGregor's 95-Mev results.

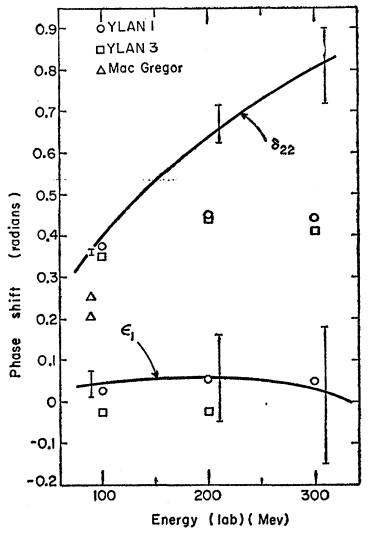

FIG. 2. The coupling parameter ϵ_1 and the uncoupled phase δ_{22}, computed from the potentials listed in Table I, are illustrated by indicating with a vertical bar the range in which they fall at three energies. The centers of these ranges are joined by a smooth curve. Two phase-shift solutions of the analysis of the data by Hull *et al.* are shown (referred to in their notation as YLAN 1 and YLAN 3), together with MacGregor's 95-Mev results.

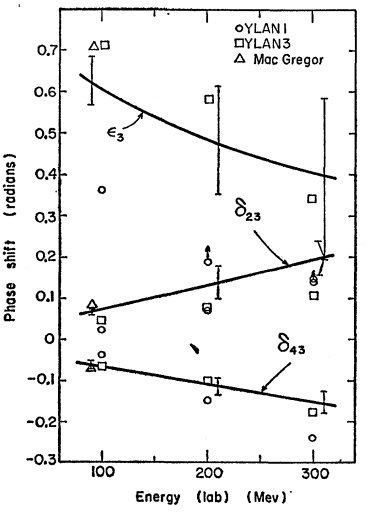

FIG. 3. The coupled phase shifts δ_{23}, δ_{43}, and coupling parameter ϵ_3, computed from the potentials listed in Table I, are illustrated by indicating with a vertical bar the range in which they fall at three energies. The centers of these ranges are joined by a smooth curve. Two phase-shift solutions of the analysis of the data by Hull *et al.* are shown (referred to in their notation as YLAN 1 and YLAN 3), together with MacGregor's 95-Mev results.

[18] J. M. Blatt and L. C. Biedenharn, Phys. Rev. **86**, 399 (1952).

TABLE V. Triplet-even phase shifts (in radians) for energies near 90 Mev (lab). These are phase shifts corresponding to potentials published by other authors. SM refers to reference 3, GT to reference 4 and H to reference 5. The phase-shift solution of MacGregor, reference 10, is also shown.

Author	E (Mev)	δ_{01}	δ_{21}	ϵ_1	δ_{23}	δ_{43}	ϵ_3	δ_{22}
SM	100	0.602	−0.293	0.059	0.11	−0.056	0.537	0.337
GT	90	0.6455	−0.230	0.0995	0.067	−0.048	0.609	0.3265
GT	300	−0.244	−0.537	0.598				0.389
H	90	0.817	−0.211	0.08	0.064	−0.058	0.77	0.22
H	200	0.415	−0.399	0.128	0.131	−0.115	0.726	0.364
H	300	0.177	−0.528	0.192	0.178	−0.148	0.690	0.432
M	95	0.721	−0.224	0.206	0.086	−0.065	0.705	0.257

increasing energy. In particular the rather large value of δ_{22} for $E=310$ Mev which we obtained for all eight potentials may have the result that the angular distribution for n-p scattering calculated from these phase shifts is in disagreement with the experimental data. This is suggested from Gammel and Thaler's analysis of n-p scattering data in terms of potentials. In this analysis the triplet-even potential was decreased in its value to make possible a fit to the 300-Mev data. Also Hamada introduced a quadratic spin-orbit force to reduce δ_{22} for 300 Mev. In Table V we have exhibited these phase shifts reported in references 3, 4, 5 and 10.

V. ELECTRON-DEUTERON ELASTIC SCATTERING

The elastic scattering of electrons from deuterons can in principle yield information about the charge and magnetic moment distribution in the deuteron and the nucleon electromagnetic form factors. It is, therefore, a process that is relevant to a study of the triplet-even force. The inelastic (deuteron-breakup) scattering however depends on the nuclear force in all states of the two-nucleon system, and therefore we reserve for a later work the study of this process.

The experimental data have been analyzed briefly by previous authors[6,7] with a view to gaining information about the triplet-even force through the deuteron charge distribution. Unfortunately only a small fraction of the deuteron volume lies within the effective range of the nucleon force, as already noted.[7] Thus, in the small-momentum-transfer region ($q\lesssim 3$ f^{-1}) we can expect that the elastic scattering is rather insensitive to the details of the inner region of the nuclear force. Therefore there is need for extending the existent measurements to higher momentum transfer in order to probe the inner region and thus possibly distinguish between the various potentials which are otherwise in agreement with the low-energy data. On the other hand we shall show that for small momentum transfer the deuteron form factor depends essentially only on the OPEP tail which is well established, and use this fact to obtain the sum of the proton and neutron charge form factor $(F_1^p+F_1^n)$ from measurements of the elastic scattering.

The theory has been developed by Jankus[6] in the first Born approximation, which should be adequate because of the small deuteron charge. The deuteron is described nonrelativistically but of course the electron is treated as a relativistic particle. His result can be written in the following modified manner, which would follow if nucleon form factors were introduced into the nucleon current operators:

$$\frac{d\sigma}{d\Omega}=\left(\frac{d\sigma}{d\Omega}\right)_0 G^2, \tag{11}$$

where

$$\left(\frac{d\sigma}{d\Omega}\right)_0=\left(\frac{e^2}{2E_0}\right)^2\frac{\cos^2(\theta/2)}{\sin^4(\theta/2)}\left(1+\frac{2E_0}{M_dc^2}\sin^2(\theta/2)\right)^{-1} \tag{12}$$

is the differential cross section for elastic scattering of an electron of energy E_0 from a point particle having no magnetic moment. The factor G^2, called the deuteron form factor, enters because of the finite extension of the deuteron and its internal constituents, the nucleons. It takes the form

$$G^2=G_0^2+G_2^2+[2\tan^2(\theta/2)+1]G_{\text{mag}}^2, \tag{13a}$$

where

$$G_0(q)=1(q^2)\int_0^\infty (u^2+w^2)j_0(qr/2)dr \tag{13b}$$

arises from the spherical part of the charge distribution,

$$G_2(q)=1(q^2)\int_0^\infty 2w(u-8^{-\frac{1}{2}}w)j_2(qr/2)dr \tag{13c}$$

is contributed by the quadrupole deformation, and

$$\begin{aligned}G_{\text{mag}}(q)=(\tfrac{2}{3})^{\frac{1}{2}}\frac{\hbar q}{2Mc}\int_0^\infty\{&[(\mu_p(q^2)+\mu_n(q^2))(u^2+w^2)\\&-\tfrac{3}{2}(\mu_p(q^2)+\mu_n(q^2)-\tfrac{1}{2}1(q^2))w^2]j_0(qr/2)\\&+2^{-\frac{1}{2}}[(\mu_p(q^2)+\mu_n(q^2))w(u+2^{-\frac{1}{2}}w)\\&+3\times 8^{-\frac{1}{2}}1(q^2)w^2]j_2(qr/2)\}dr\end{aligned} \tag{13d}$$

is the magnetic moment contribution. In the above formula M_d is the deuteron mass, M is the nucleon mass and q is the four-momentum transfer. Actually in the nonrelativistic treatment of the deuteron the three-momentum transfer appears in the argument of the spherical Bessel functions in Eqs. (13). But considera-

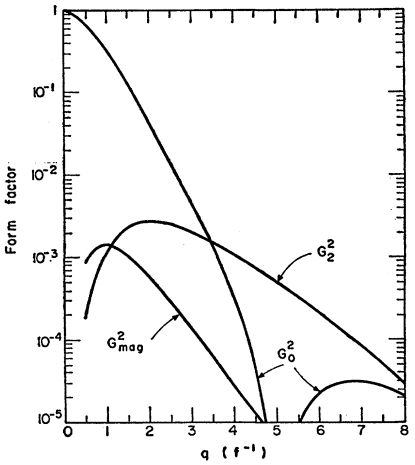

FIG. 4. The spherical, quadrupole, and magnetic moment parts of the deuteron electromagnetic form factor calculated from potential No. 2 (Table I) are shown. The nucleon form factors of Hofstadter and Herman have been used (reference 21).

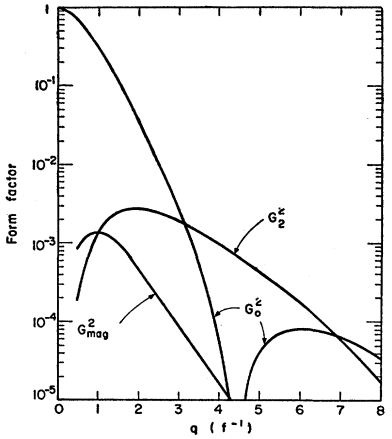

FIG. 5. The spherical, quadrupole, and magnetic moment parts of the deuteron electromagnetic form factors calculated from potential No. 3 (Table I) are shown. The nucleon form factors of Hofstadter and Herman have been used (reference 21).

tions on the basis of perturbation theory suggest that in a relativistic theory this three-momentum is replaced by the four-momentum.

For structureless nucleons the functions $1(q^2)$, $\mu_n(q^2)$, and $\mu_p(q^2)$ take, respectively, the value unity and the values of the nucleon magnetic moments μ_n and μ_p. Otherwise they are

$$\begin{aligned} 1(q^2)&=F_1^n(q^2)+F_1^p(q^2),\\ \mu_p(q^2)&=F_1^p(q^2)+(\mu_p-1)F_2^p(q^2),\\ \mu_n(q^2)&=F_1^n(q^2)+\mu_nF_2^n(q^2), \end{aligned} \tag{14}$$

where F_1^p, F_2^p, F_1^n, F_2^n are the nucleon form factors, defined as usual.[19] One notices that the elastic electron-deuteron cross section depends only on the sum of the proton and neutron form factors, characteristic of a state with isotopic spin $T=0$.

Quite reliable measurements of the proton form factors are available.[20] However, the neutron form factors cannot be obtained directly, and are in practice extracted from the electron-deuteron inelastic scattering cross section. So far no complete calculation including the D-state admixture and all the final-state interactions has been carried out for this process.

We have computed the deuteron form factor G^2 corresponding to most of the potentials listed in Tables I and II. The three parts of G^2 are illustrated in Figs. 4 and 5 for two of our potentials. For purposes of illustration we have used the nucleon form factors given by Hofstadter and Herman.[21] The magnetic moment term, G_{mag}^2, is almost everywhere smaller by two orders of magnitude than the other terms. Therefore, except for very-large-angle scattering, G_{mag}^2 contributes only in the third figure of G^2. Our calculations of the deuteron form factor G^2 are summarized in Fig. 6 by showing the boundaries between which all form factors corresponding to our potentials fall (except that form factors for No. 5 and No. 7 have not been calculated). It is particularly noteworthy that these bounds lie close together for small momentum transfer. The break in the slope that occurs around $q=3.5$ f^{-1} corresponds to the point where the quadrupole term begins to dominate G^2. We can see from Figs. 4 and 5 that the spherical term will again commence to dominate at $7\lesssim q\lesssim 9$ f^{-1}, and there will be another break in the slope of G^2. However, the location of this break is much more dependent on the details of the force at small distance than the location of the first break. Indeed, already at $q=7$ f^{-1}, the un-

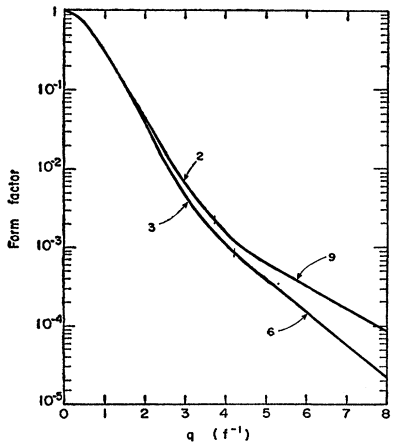

FIG. 6. The two curves represent the upper and lower bounds on the deuteron electromagnetic form factor as calculated from the potentials in Table I (excluding Nos. 5 and 7, which have not been calculated). For purposes of illustration we have used a constant scattering angle $\theta=90°$. The numbers on the curves correspond to the potential numbers in Table I. The nucleon form factors of Hofstadter and Herman have been used (reference 21).

[19] See, for example, the review article by R. Hofstadter, Ann. Rev. Nuclear Sci. 7, 231 (1957).

[20] F. Bumiller, M. Croissiaux, E. Dally, and R. Hofstadter, Phys. Rev. 124, 1623 (1961).

[21] R. Hofstadter and R. Herman, Phys. Rev. Letters 6, 293 (1961). Eqs. (9) throughout (12) were used for the form factors.

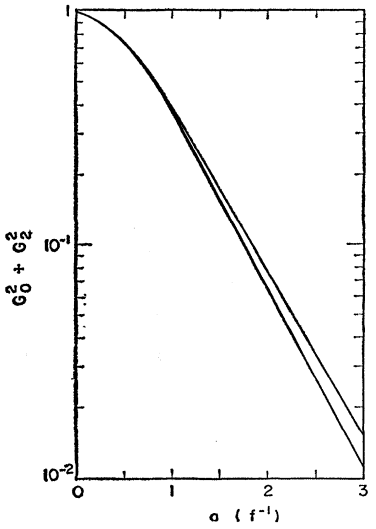

FIG. 7. The sum of the spherical and quadrupole parts of the deuteron form factor for point nucleons [$1(q^2)=1$], is illustrated in the momentum-transfer region in which lie the current experimental results on elastic electron-deuteron scattering. The two curves correspond to the upper and lower values of this sum that are given by the potentials listed in Table I (except that Nos. 5 and 7 have not been calculated). The upper curve corresponds to potential No. 2 and the lower to No. 3.

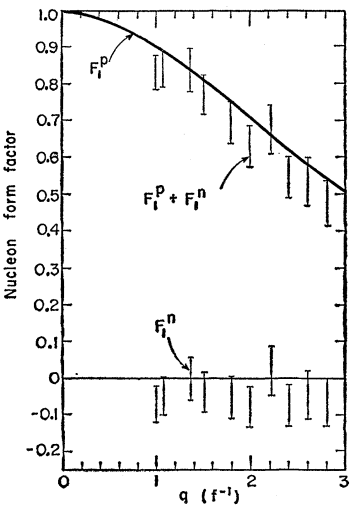

FIG. 8. The sum of the charge parts of the nucleon form factors $F_1^n+F_1^p$ which is deduced from Eq. (15) is shown. At $q\approx 1$ f^{-1} about 20%, and at $q\approx 3$ f^{-1} about 50%, of the spread is due to our incomplete knowledge of the triplet-even force. The rest is experimental error in the elastic scattering experiment. The proton charge form factor F_1^p is obtained from reference 20 by drawing a smooth curve through the experimental results. There is an error on this curve of about ± 0.03. The neutron charge form factor is obtained by subtracting the smoothed proton data from the points for $F_1^p+F_1^n$. The error on the proton form factor should be added to those already shown on F_1^n to get the total uncertainty.

certainty in G^2 due to our incomplete knowledge of the n-p force at small distance can be as large as a factor of 3. In particular the potential No. 6 which gives rise to a node in the D function, as discussed in Sec. III, gives a G^2 which lies below all the others by a factor of 2 at $q=7$ f^{-1}. The region $q\gtrsim 7$ f^{-1} is therefore appropriate for studying the inner region of the potential.

Using our calculations of the deuteron form factors, we can extract the sum of the neutron and proton charge form factors $F_1^n+F_1^p$ for $q\lesssim 3$ f^{-1} from the experimental data on elastic electron-deuteron scattering,[22] in a manner that involves practically no theoretical uncertainty arising from our incomplete knowledge of the n-p force. This is because, in the range of q for which we have experimental measurements of G^2, the integrals that enter the calculation depend almost solely on that part of the n-p force which is well established, that is, the OPEP tail. This can be seen explicitly in Fig. 7, where upper and lower bounds of $G_0^2+G_2^2$ are exhibited.

The extraction of the scalar charge form factor, $F_1^n+F_1^p$, is accomplished through use of the equation

$$G_{\rm exp}^2=(F_1^n+F_1^p)^2(G_0^2+G_2^2)+[2\tan^2(\theta/2)+1]G_{\rm mag}^2. \quad (15)$$

On the left side we insert the experimental quantity $(d\sigma/d\Omega)_{\rm exp}/(d\sigma/d\Omega)_0$. On the right G_0^2 and G_2^2 are obtained from Eqs. (13b and c) with $1(q^2)\to 1$. The magnetic term does not contain $F_1^n+F_1^p$ as a multiplicative factor, and moreover contains the magnetic parts of the nucleon form factors [Eq. (13d)]. However, as can be seen from Figs. 4 and 5, this term affects only the third figure of G^2. It is reasonable to assume that the already published values of the nucleon form factors will allow us to compute $G_{\rm mag}$ to at least one significant figure. Therefore in $G_{\rm mag}$ we insert the nucleon form factors of reference 21.

Our results for $F_1^n+F_1^p$ are shown in Fig. 8. The upper bound is obtained by using the maximum experimental value of $G_{\rm exp}^2$ and the minimum value of $G_0^2+G_2^2$ obtained from theory, and similarly for the lower bound.

We have subtracted a smooth curve drawn through recent experimental measurements[20] of F_1^p to obtain the neutron charge form factor F_1^n. These results are illustrated in Fig. 8, and have been tabulated earlier.[23] As can be seen from this figure, it is consistent with the experimental data to say that the neutron-charge form factor F_1^n is zero, at least up to momentum transfer $q=3$ f^{-1}. However, most of the points suggest that F_1^n may have a very small negative value in this region. These results are in disagreement with those of reference 8 where small positive values are reported, obtained from an analysis of the inelastic electron-deuteron scattering data. The data have been reanalyzed by Durand[24] who obtained values of F_1^n generally smaller than those reported in reference 8, and possibly negative in sign.

[22] J. I. Friedman, H. W. Kendall, and P. A. M. Gram, Phys. Rev. **120**, 992 (1960).

[23] N. K. Glendenning and G. Kramer, Phys. Rev. Letters **7**, 471 (1961).

[24] L. Durand III, Phys. Rev. Letters **6**, 631 (1961). See footnote 15 of this reference. The theory on which Durand's calculation is based is given in more detail in his later work; Phys. Rev. **123**, 1393 (1961).

TABLE VI. The four integrals that enter the calculation of the deuteron electromagnetic form factor for some of the potentials of Table I. Each quantity is arbitrarily truncated after the fifth figure and is followed by the exponent to the base 10.

q (f^{-1})	$\int u^2 j_0$	$\int w^2 j_0$	$\int uwj_2$	$\int w^2 j_2$
		Potential No. 1		
0.5000	7.9453-01	7.0119-02	7.8766-03	1.5756-03
1.0000	5.5698-01	6.0193-02	2.2664-02	5.1242-03
1.5000	3.6076-01	4.8109-02	3.4480-02	8.8252-03
2.0000	2.2497-01	3.6383-02	4.0997-02	1.1683-02
2.5000	1.3512-01	2.6199-02	4.3052-02	1.3422-02
3.0000	7.6529-02	1.7921-02	4.2043-02	1.4129-02
3.5000	3.8736-02	1.1491-02	3.9168-02	1.4022-02
4.0000	1.4770-02	6.6764-03	3.5300-02	1.3338-02
		Potential No. 2		
0.5000	8.0624-01	5.9029-02	7.6826-03	1.4724-03
1.0000	5.6936-01	4.9823-02	2.2005-02	4.7455-03
1.5000	3.7363-01	3.8790-02	3.3251-02	8.0652-03
2.0000	2.3808-01	2.8315-02	3.9194-02	1.0500-02
2.5000	1.4820-01	1.9471-02	4.0738-02	1.1827-02
3.0000	8.9347-02	1.2527-02	3.9325-02	1.2171-02
3.5000	5.1075-02	7.3571-03	3.6177-02	1.1778-02
4.0000	2.6439-02	3.6794-03	3.2174-02	1.0897-02
4.5000	1.0844-02	1.1835-03	2.7897-02	9.7401-03
5.0000	1.2478-03	−4.2067-04	2.3701-02	8.4626-03
5.5000	−4.3898-03	−1.3728-03	1.9794-02	7.1767-03
6.0000	−7.4366-03	−1.8648-03	1.6279-02	5.9545-03
6.5000	−8.8138-03	−2.0440-03	1.3197-02	4.8385-03
7.0000	−9.1415-03	−2.0200-03	1.0546-02	3.8498-03
7.5000	−8.8350-03	−1.8724-03	8.3030-03	2.9950-03
8.0000	−8.1706-03	−1.6572-03	6.4298-03	2.2713-03
		Potential No. 3		
0.5000	8.0435-01	5.6096-02	7.6440-03	1.4055-03
1.0000	5.5885-01	4.7319-02	2.1844-02	4.5235-03
1.5000	3.5686-01	3.6818-02	3.2905-02	7.6770-03
2.0000	2.1803-01	2.6863-02	3.8645-02	9.9841-03
2.5000	1.2714-01	1.8462-02	4.0000-02	1.1239-02
3.0000	6.8761-02	1.1862-02	3.8428-02	1.1567-02
3.5000	3.1894-02	6.9391-03	3.5155-02	1.1201-02
4.0000	9.1906-03	3.4267-03	3.1056-02	1.0376-02
4.5000	−4.2191-03	1.0326-03	2.6706-02	9.2884-03
5.0000	−1.1568-02	−5.1311-04	2.2458-02	8.0838-03
5.5000	−1.5018-02	−1.4355-03	1.8516-02	6.8667-03
6.0000	−1.6014-02	−1.9147-03	1.4982-02	5.7046-03
6.5000	−1.5523-02	−2.0895-03	1.1894-02	4.6381-03
7.0000	−1.4187-02	−2.0640-03	9.2519-03	3.6880-03
7.5000	−1.2430-02	−1.9147-03	7.0288-03	2.8620-03
8.0000	−1.0523-02	−1.6960-03	5.1883-03	2.1585-03
		Potential No. 4		
0.5000	7.9823-01	6.7169-02	7.7092-03	1.5094-03
1.0000	5.6163-01	5.7672-02	2.2167-02	4.9019-03
1.5000	3.6602-01	4.6135-02	3.3698-02	8.4264-03
2.0000	2.3043-01	3.4968-02	4.0042-02	1.1133-02
2.5000	1.4045-01	2.5294-02	4.2034-02	1.2768-02
3.0000	8.1521-02	1.7444-02	4.1052-02	1.3421-02
3.5000	4.3258-02	1.1351-02	3.8272-02	1.3307-02
4.0000	1.8749-02	6.7870-03	3.4543-02	1.2655-02
4.5000	3.4153-03	3.4743-03	3.0431-02	1.1660-02
5.0000	−5.7977-03	1.1506-03	2.6296-02	1.0478-02
5.5000	−1.0941-02	−4.1332-04	2.2354-02	9.2226-03
6.0000	−1.3406-02	−1.4068-03	1.8724-02	7.9705-03
6.5000	−1.4139-02	−1.9813-03	1.5463-02	6.7743-03
7.0000	−1.3784-02	−2.2552-03	1.2589-02	5.6657-03
7.5000	−1.2783-02	−2.3195-03	1.0094-02	4.6619-03
8.0000	−1.1431-02	−2.2430-03	7.9562-03	3.7699-03
		Potential No. 6		
0.5000	8.0861-01	5.5848-02	7.6481-03	1.4492-03
1.0000	5.7013-01	4.6804-02	2.1864-02	4.6604-03
1.5000	3.7309-01	3.6010-02	3.2934-02	7.8921-03
2.0000	2.3667-01	2.5832-02	3.8634-02	1.0221-02
2.5000	1.4628-01	1.7330-02	3.9874-02	1.1430-02
3.0000	8.7167-02	1.0762-02	3.8106-02	1.1649-02
3.5000	4.8829-02	5.9908-03	3.4567-02	1.1127-02
4.0000	2.4261-02	2.7225-03	3.0152-02	1.0122-02
4.5000	8.8267-03	6.3134-04	2.5462-02	8.8521-03
5.0000	−5.5656-04	−5.8370-04	2.0873-02	7.4811-03
5.5000	−5.9533-03	−1.1767-03	1.6607-02	6.1271-03
6.0000	−8.7535-03	−1.3508-03	1.2782-02	4.5666-03
6.5000	−9.8943-03	−1.2615-03	9.4466-03	3.7446-03
7.0000	−1.0006-02	−1.0237-03	6.6044-03	2.7829-03
7.5000	−9.5136-03	−7.1927-04	4.2337-03	1.9867-03
8.0000	−8.6937-03	−4.0405-04	2.2970-03	1.3503-03
		Potential No. 8		
0.5000	8.1020-01	5.2586-02	7.6488-03	1.4144-03
1.0000	5.6855-01	4.3785-02	2.1839-02	4.5327-03
1.5000	3.6890-01	3.3339-02	3.2845-02	7.6400-03
2.0000	2.3070-01	2.3559-02	3.8481-02	9.8429-03
2.5000	1.3919-01	1.5451-02	3.9698-02	1.0947-02
3.0000	7.9454-02	9.2328-03	3.7975-02	1.1099-02
3.5000	4.0841-02	4.7432-03	3.4560-02	1.0556-02
4.0000	1.6268-02	1.6794-03	3.0341-02	9.5733-03
4.5000	1.0401-03	−2.8202-04	2.5903-02	8.3582-03
5.0000	−7.9702-03	−1.4317-03	2.1601-02	7.0663-03
5.5000	−1.2863-02	−2.0088-03	1.7637-02	5.8023-03
6.0000	−1.5058-02	−2.1998-03	1.4109-02	4.6318-03
6.5000	−1.5521-02	−2.1443-03	1.1050-02	3.5902-03
7.0000	−1.4907-02	−1.9436-03	8.4527-03	2.6925-03
7.5000	−1.3662-02	−1.6685-03	6.2874-03	1.9396-03
8.0000	−1.2086-02	−1.3671-03	4.5123-03	1.3238-03
		Potential No. 9		
0.5000	7.9455-01	7.0352-02	7.7304-03	1.5218-03
1.0000	5.5728-01	6.0763-02	2.2235-02	4.9509-03
1.5000	3.6139-01	4.9076-02	3.3819-02	8.5348-03
2.0000	2.2594-01	3.7707-02	4.0217-02	1.1320-02
2.5000	1.3641-01	2.7789-02	4.2266-02	1.3045-02
3.0000	7.8084-02	1.9665-02	4.1343-02	1.3795-02
3.5000	4.0485-02	1.3282-02	3.8620-02	1.3776-02
4.0000	1.6632-02	8.4232-03	3.4944-02	1.3213-02
4.5000	1.9030-03	4.8221-03	3.0879-02	1.2296-02
5.0000	−6.7812-03	2.2246-03	2.6784-02	1.1177-02
5.5000	−1.1482-02	4.0808-04	2.2872-02	9.9670-03
6.0000	−1.3593-02	−8.1274-04	1.9263-02	8.7438-03
6.5000	−1.4055-02	−1.5868-03	1.6013-02	7.5597-03
7.0000	−1.3504-02	−2.0316-03	1.3139-02	6.4474-03
7.5000	−1.2370-02	−2.2385-03	1.0636-02	5.4260-03
8.0000	−1.0940-02	−2.2776-03	8.4813-03	4.5044-03

There is some uncertainty introduced into our results by unknown relativistic and meson-current effects. However we feel that these effects will be small in the region of low momentum transfer considered here.[25]

To facilitate the analysis of future measurements of elastic electron-deuteron scattering we give in Table VI

[25] R. Blankenbecler, thesis, Stanford University, 1958, has studied relativistic corrections, using a simplified model of the deuteron (two bosons, one of which is charged, bound by a separable potential). In this model the corrections can give rise to a 25 to 30% reduction in the cross section at $q=3$ f^{-1} which would mean that the scalar charge form factor would be larger by as much as 15%. Whether the corrections would be as large, in a realistic model is not clear. However, suppose that this is the correction that obtains at $q=3$ f^{-1}. Then if we applied a correction that is 15% at $q=3$ f^{-1} and goes linearly to zero as $q\to 0$, the limits we place on F_1^n would lie one above and one below the zero value for all values of q listed in our table except at $q=2.2$ f^{-1}, where both limits are positive.

the four types of integrals that enter G^2, calculated from some of our potentials, for momentum transfer up to $q=8$ f^{-1}.

Note added in proof. We are indebted to Dr. H. P. Noyes for informing us that the triplet scattering length is now known much more accurately than indicated by the sources we quoted. Based on a very careful study of the experimental data, R. Wilson in a book on nucleon-nucleon scattering [Interscience Publishers, Inc., New York (to be published)] reports a value of the n-p cross section at a few ev of 20.400 ± 0.060 barns and a coherent scattering length of -3.744 ± 0.010 f. Therefore the triplet and singlet scattering lengths are: $a_t=5.4043\pm0.0122$ f and $a_s=-23.7009\pm0.0332$ f. Hence potential No. 8 is the only one which now fits the experimental data.

The deuteron binding energy is also known more accurately now and the weighted mean of the experimental values is 2224.68 ± 0.196 kev.

ACKNOWLEDGMENTS

One of us (G.K.) expresses his appreciation to Professor I. Perlman and Professor J. O. Rasmussen for their hospitality. An IBM 709 computer at this laboratory was used to perform the calculations.

PHYSICAL REVIEW VOLUME 126, NUMBER 6 JUNE 15, 1962

Gamma Rays Resulting from Lithium Bombardments of Lithium*

EDWARD H. BERKOWITZ

Department of Physics and Astronomy, State University of Iowa, Iowa City, Iowa

(Received July 17, 1961)

Lithium beams of mass 6 and 7 were used to bombard thick targets of Li^6F and Li^7F. Reactions leading to Li^7, Be^7, Be^{10}, B^{10}, B^{11}, B^{12}, C^{11}, C^{12}, and C^{13} were identified from direct observation of gamma rays, residual target radiation, and the presence of neutrons.

I. EXPERIMENTAL APPARATUS

THICK targets of Li^6F and Li^7F were bombarded by 2.5–2.75-Mev Li^6 and Li^7 beams obtained from the State University of Iowa Van de Graaff accelerator. The ion source is of the hot filament type and is similar to one described by Norbeck[1] and Allison and Littlejohn.[2] Gamma rays from these reactions were

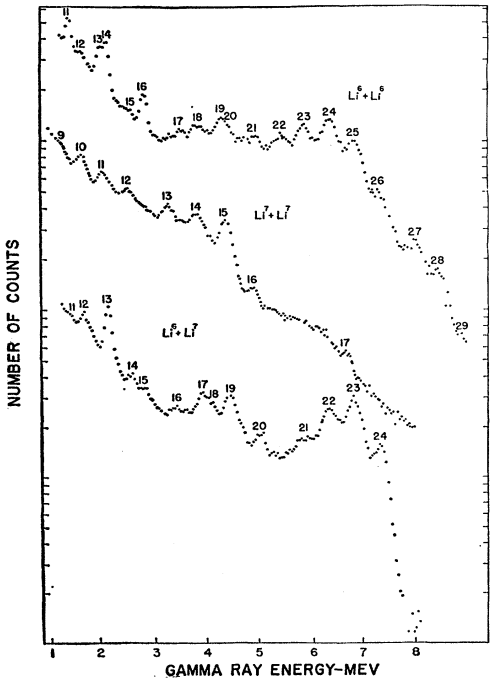

FIG. 1. High-energy spectra. Most peaks contain more than 10^3 counts per point. Ordinates are arbitrary and different for each of the three curves.

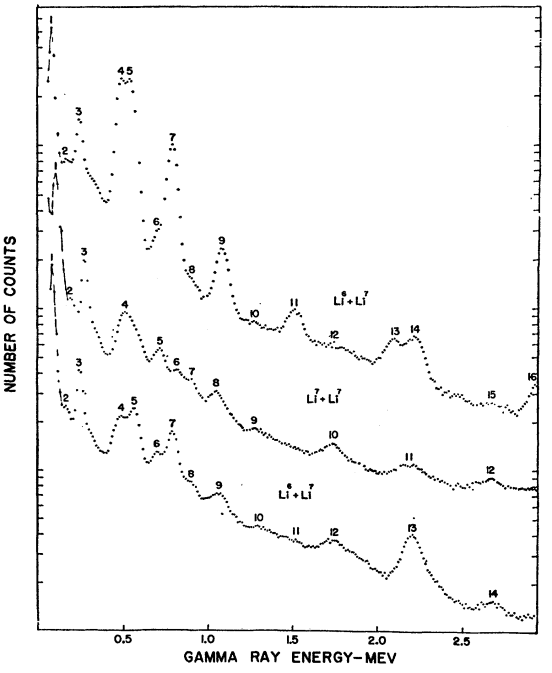

FIG. 2. Low-energy spectra. Most peaks contain more than 10^3 counts per point. Ordinates are arbitrary and different for each of the three curves.

* Supported in part by the U. S. Atomic Energy Commission.

[1] E. Norbeck, Jr., Phys. Rev. **105**, 204 (1957).

[2] S. K. Allison and C. S. Littlejohn, Phys. Rev. **104**, 959 (1956).